Magnetic Control of Dual-Spin and Bias Momentum Spacecraft

Anton H. J. de Ruiter *

Carleton University

1125 Colonel By Drive, Ottawa, ON K1S 5B6, Canada

aderuite@mae.carleton.ca

Abstract

This paper examines simultaneous attitude control and momentum wheel management of dual-spin and bias momentum spacecraft utilizing magnetic actuation. Transformations of variables are presented leading to the derivation of control laws yielding proven stability and asymptotic convergence under appropriate assumptions on the Earth's magnetic field. The results remain valid in the presence of magnetic torquer saturation. Furthermore, it is shown that for a spacecraft equipped with three orthogonal magnetic torquers, the control laws are tolerant to the failure of a single magnetic torquer in the case of a dual-spin spacecraft, and tolerant to the failure of two magnetic torquers in the case of a bias momentum spacecraft provided the remaining magnetic torquer does not generate its dipole moment parallel to the momentum wheel spin axis. Additionally, the stability analyses show that the control laws remain stabilizing under the effects of control quantization. The theoretical results rely on the assumption that the spacecraft principal and body axes coincide. Robustness to uncertainties in the spacecraft inertia matrix, and to disturbance torques are demonstrated with a numerical example.

1 Introduction

Dual-spin and bias momentum configurations are well established passive stabilization techniques for spacecraft, and have been proven on orbit [1, sect.6.7, ch. 8], [2, sect. 18.2]. Due to the presence of disturbances, the passively stable dual-spin and bias momentum configurations must be augmented with some active stabilization, serving two purposes. The first is to damp nutational and precessional motion, the second is to manage stored angular momentum in the momentum wheel. One actuation scheme for the active stabilization of dual-spin and bias momentum spacecraft makes use of magnetic torquers. Magnetic torquers do not contain any moving parts, and prove to a very reliable

*Anton de Ruiter is an Assistant Professor at Carleton University

means of actuation. There has been a significant amount of research performed in the area of magnetic control of bias momentum spacecraft, using various approaches [3, 4, 5, 6, 7, 9]. In [3] and [4], the Earth's magnetic field as seen on orbit is assumed to be periodic, and time-invariant approximations of the linearized equations of motion (for a bias momentum spacecraft) are obtained to study the stability properties of the presented control laws. In [5], [6] and [7], the Earth's magnetic field is again assumed to be periodic, and LQ-type periodic optimal control theory is applied to the linearized equations of motion for a bias momentum spacecraft. In [8], a magnetically controlled bias momentum spacecraft is considered. A PD-type control law is designed with the use of genetic algorithms to obtain a stabilizing control law using only two magnetic torquers. None of the stability results in the afore-mentioned papers have any guarantees under actuator saturation. In [9], a model predictive control approach is taken to develop magnetic control laws for a bias momentum spacecraft. It is shown in [9] how actuator saturation constraints can be included in the formulation of the control law. However, there are no guarantees for the resulting closed-loop system stability, and stability must be checked after the fact.

There are several other magnetic attitude control techniques in the literature for spacecraft that are not necessarily bias momentum or dual-spin. In [10] and [11], ideal control laws are initially designed, assuming full three-axis actuation. These ideal control laws are then implemented magnetically by projecting the ideal control torque onto the plane normal to the local Earth's magnetic field. Stability of the closed-loop system is then checked after the fact. In [10], average coefficient analysis is used with the linearized equations of motion to estabilish stability. In [11], stability is established using a Lyapunov-type analysis with the linearized equations of motion. In neither of these methods are there any stability guarantees under actuator saturation. In [12], two approaches are presented. In both approaches, the Earth's magnetic field is approximated as periodic. In the first approach, finite and infinite horizon LQ-type periodic optimal control theory is applied to the linearized equations of motion. In the second approach, a LQ-type optimal control theory is applied to a time-invariant approximation of the linearized equations of motion, thereby obtaining a constant gain controller. Stability is checked for the constant gain controller after the fact using Floquet analysis. There are no guarantees in either approach for stability under actuator saturation. In [13], the Earth's magnetic field is initially approximated as periodic. The linearized equations of motion are considered with LQ-type periodic optimal control theory. A time-invariant approximation to the resulting steady-state solution of the periodic Riccati equation is obtained, resulting in a control law that is easy to implement, and requires only a measurement of the local Earth's magnetic field rather than a-priori knowledge of it. However, there are no guarantees of stability, which must be checked after the fact using for example Floquet analysis. In [13], a method is also presented to deal with actuator saturation. When the attitude error is large, the control gain is reduced such that the actuators do not saturate. When the attitude error is small, the gain is increased to speed up convergence.

The afore-mentioned references all present local results. There are also global treatments in the literature. In [14] and [15], the Earth's magnetic field is assumed to be periodic, allowing the authors to obtain globally stable

magnetic attitude control laws using Krasovskii-LaSalle type analysis. However, there are no guarantees under actuator saturation. References [16], [17] and [18] do not make any assumptions on the periodicity of the Earth's magnetic field, and utilize generalized averaging theory to obtain globally stable magnetic attitude controllers. The resulting controllers have small gain limitations. There is no analytical method for determining upper limits on the controller gains, and tuning must be used. Reference [17] demonstrates how the control law may be modified to account for actuator saturation with guaranteed stability. In [19] and [20] magnetic actuation is augmented with mechanical actuation. Passivity-based arguments are then used to obtain globally stable controllers, with no limitations on the magnitude of the gains. There are however, no guarantees of stability under actuator saturation.

In this paper, the magnetic control of dual-spin spacecraft with a despun platform, and a bias momentum spacecraft are considered. In both cases, a transformation of variables with the linearized equations of motion are used to develop magnetic control laws to simultaneously control roll and yaw attitude motion as well as manage the stored angular momentum in the pitch momentum wheel. No assumption is made on the periodicity of the Earth's magnetic field. The resulting control laws have the form such that they are the projection of ideal control laws (assuming full three axis actuation) onto the plane normal to the Earth's magnetic field. Using a similar approach as in [21], it is demonstrated that the resulting control laws are locally stable and convergent, even under the effects of magnetic torquer saturation and the failure of a single magnetic torquer in the case of a dual-spin spacecraft, or the failure of two magnetic torquers in the case of a bias momentum spacecraft provided the remaining magnetic torquer does not generate its dipole moment parallel to the momentum wheel spin axis. As such, the ideal control law may be designed first, with closed-loop stability and convergence guaranteed when implemented magnetically. It must be noted that the theoretical results in this paper are valid only when the spacecraft principal and body axes coincide. Robustness to variations in the spacecraft inertia matrix must be determined numerically. A numerical example is presented, demonstrating robustness of the algorithms to spacecraft inertia matrix uncertainties, as well as disturbance torques.

2 Notational and Mathematical Preliminaries

The identity matrix is denoted by $\mathbf{1}$ so as to distinguish it from the spacecraft inertia matrix. The cross-product operator matrix associated with a vector $\mathbf{a} = \begin{bmatrix} a_x & a_y & a_z \end{bmatrix}^T \in R^3$ is given by

$$\mathbf{a}^\times = \begin{bmatrix} 0 & -a_z & a_y \\ a_z & 0 & -a_x \\ -a_y & a_x & 0 \end{bmatrix}.$$

We take the norm $||\mathbf{x}||$ of a vector $\mathbf{x}$ to mean the usual Euclidean norm.

Proposition 1

Let $D \subset R^n$ be a domain, and let $\boldsymbol{\phi}(\mathbf{x}) : D \to R^m$ be continuous on D. Let $\mathbf{x}(t) : R \to R^n$ be such that $\mathbf{x}(t) \in H$ for $t \geq 0$ where H is a compact subset of D. Additionally, define the set $G \triangleq \{\mathbf{x} \in R^n : \boldsymbol{\phi}(\mathbf{x}) = 0\}$.

Suppose that

$$\lim_{t \to \infty} \boldsymbol{\phi}(\mathbf{x}(t)) = \mathbf{0}.$$

Then, $\mathbf{x}(t)$ approaches the set G as $t \to \infty$.

Proof

Recall that the distance of a point $\mathbf{y} \in R^n$ to the set G is defined as $\text{dist}(\mathbf{y}, G) \triangleq \inf_{x \in G} ||\mathbf{y} - \mathbf{x}||$. Now, let us define the set $J \triangleq \{\mathbf{x} \in R^n : \text{dist}(\mathbf{x}, G) \geq \eta\}$, for some $\eta > 0$. Clearly, $J \cap G = \emptyset$. It is also readily demonstrated that J is closed. Now, consider the set $F \triangleq H \cap J$. Since both H and J are closed, and H is bounded, F is compact. Since $\boldsymbol{\phi}(\mathbf{x})$ is continuous, $||\boldsymbol{\phi}(\mathbf{x})||$ achieves its maximum and minimum on F. That is, let $\epsilon = \inf_{\mathbf{x} \in F} ||\boldsymbol{\phi}(\mathbf{x})||$, then $\exists \mathbf{y} \in F$ such that $||\boldsymbol{\phi}(\mathbf{y})|| = \epsilon$. It must be that $\epsilon > 0$, since if $\epsilon = 0$, then $\boldsymbol{\phi}(\mathbf{y}) = \mathbf{0}$, which implies that $\mathbf{y} \in G$, which is a contradiction since $F \cap G = \emptyset$.

Now, to prove the assertion in the lemma, assume that $\mathbf{x}(t)$ a does not approach the set G as $t \to \infty$. Then, $\exists \eta > 0$ and a sequence $t_k \to \infty$ as $k \to \infty$ such that $\text{dist}(\mathbf{x}(t_k), G) \geq \eta$ for all $k \geq 0$. Since we know that $\mathbf{x}(t) \in H$ for $t \geq 0$, this implies that $\mathbf{x}(t_k) \in F$. From above, this implies that $\boldsymbol{\phi}(\mathbf{x}(t_k)) \geq \epsilon > 0$ for all $k \geq 0$. This contradicts the convergence of $\boldsymbol{\phi}(\mathbf{x}(t)) \to \mathbf{0}$ as $t \to \infty$. Therefore, it must be that $\mathbf{x}(t)$ approaches the set G as $t \to \infty$. □

The following Theorem from [22] will also be made use of.

Theorem 1 [22, p. 62]

Consider the systems

$$\dot{\mathbf{x}} = \mathbf{g}(\mathbf{x}), \tag{1}$$

and

$$\dot{\mathbf{x}} = \mathbf{f}(\mathbf{x}, t), \;\; \mathbf{x}(0) = \mathbf{x}_0. \tag{2}$$

where $\mathbf{x} \in R^n$, $t \in R$. We assume that there is a domain $D_o \subset R^n$ such that $\mathbf{g}(\mathbf{x}) \in C(D_o)$ and $\mathbf{f}(\mathbf{x}, t) \in C(D_o \times R)$, and that $\mathbf{f}(\mathbf{x}, t) \to \mathbf{g}(\mathbf{x})$ uniformly in $\mathbf{x}$ on compact subsets of D_o as $t \to \infty$.

Suppose that there exists a solution $\boldsymbol{\phi}(t)$ of (2) and a compact subset $D_1 \subset D_o$, such that $\boldsymbol{\phi}(t) \in D_1$ for all $t \geq 0$.

Then, given any sequence $t_m \to \infty$, there exists a subsequence $\{t_{m_j}\}$ and a solution $\boldsymbol{\psi}(t)$ of (1) such that

$$\boldsymbol{\phi}(t + t_{m_j}) \to \boldsymbol{\psi}(t), \text{ as } m_j \to \infty,$$

uniformly in t on compact subsets of R.

3 Spacecraft Attitude Dynamics

In body coordinates, the attitude dynamics of a spacecraft containing momentum wheels are [23, pp.157, 237]

$$\mathbf{I}\dot{\boldsymbol{\omega}} = -\boldsymbol{\omega}^{\times}(\mathbf{I}\boldsymbol{\omega} + \mathbf{h}_w) - \dot{\mathbf{h}}_w + \boldsymbol{\tau}_c + \boldsymbol{\tau}_d, \tag{3}$$

where $\mathbf{I}$ is the spacecraft inertia matrix, $\boldsymbol{\omega}$ is the inertial angular velocity, $\mathbf{h}_w$ is the total stored angular momentum in the wheels, $\boldsymbol{\tau}_c$ is a control torque provided by actuators other than the wheels, such as magnetic torquers or thrusters, and $\boldsymbol{\tau}_d$ is an external disturbance torque.

We assume that the spacecraft body frame is a principal axes frame, and that as a result the spacecraft inertia matrix has the form

$$\mathbf{I} = \begin{bmatrix} I_x & 0 & 0 \\ 0 & I_y & 0 \\ 0 & 0 & I_z \end{bmatrix}.$$

Since we are considering dual-spin and bias momentum spacecraft, the spacecraft has a single momentum wheel and we take the spin axis as coinciding with the spacecraft pitch axis. Therefore, the stored angular momentum vector has the form

$$\mathbf{h}_w = \begin{bmatrix} 0 \\ h_w \\ 0 \end{bmatrix}.$$

For the control law development and stability analysis, we shall consider the disturbance-free attitude equations, that is we set $\boldsymbol{\tau}_d = \mathbf{0}$.

3.1 Dual-Spin Spacecraft

We consider a dual-spin spacecraft with a de-spun platform. We describe the spacecraft inertial attitude by roll (ϕ), pitch (θ), and yaw (ψ) Euler angles (since we will consider only small angles, the order of rotations is irrelevant). For small angles and rates, the disturbance-free attitude equations of motion (3) become

$$\begin{aligned} I_x\ddot{\phi} &= h_w\dot{\psi} + \tau_{c,x}, \\ I_y\ddot{\theta} &= -\dot{h}_w + \tau_{c,y}, \\ I_z\ddot{\psi} &= -h_w\dot{\phi} + \tau_{c,z}. \end{aligned} \tag{4}$$

The available control inputs are $\boldsymbol{\tau}_c$ and $\dot{h}_w$.

3.2 Bias-Momentum Spacecraft

We assume that the spacecraft is in a circular orbit, and we describe the spacecraft attitude relative to a local orbiting frame by roll (ϕ), pitch (θ), and yaw (ψ) Euler angles (as in the dual-spin case, since we will consider only small angles, the order of rotations is irrelevant). For small angles and rates, the attitude equations of motion including the gravity-gradient torque (3) become

$$\begin{aligned} I_x\ddot{\phi} - a\dot{\psi} - b\phi &= \tau_{c,x}, \\ I_y\ddot{\theta} + 3(I_x - I_z)\omega_o^2\theta &= -\dot{h}_w + \tau_{c,y}, \\ I_z\ddot{\psi} + a\dot{\phi} - c\psi &= \tau_{c,z}, \end{aligned} \tag{5}$$

where

$$a = (I_x + I_z - I_y)\,\omega_o + h_w,\ \ b = \omega_o h_w - 4\,(I_y - I_z)\,\omega_o^2,\ \ c = \omega_o h_w - (I_y - I_x)\,\omega_o^2,$$

where ω_o is the orbital angular rate. The available control inputs are $\boldsymbol{\tau}_c$ and $\dot{h}_w$.

4 Attitude Control and Stability Analysis

4.1 Dual-Spin Spacecraft

It is clear from (4) that the roll and yaw equations can be decoupled from the pitch equation. We do this by selecting the pitch control law

$$\dot{h}_w = k_{pp}\theta + k_{dp}\dot{\theta} + \tau_{c,y}, \tag{6}$$

with $k_{pp} > 0$ and $k_{dp} > 0$ proportional and derivative gains respectively. That is, we use the momentum wheel to control the pitch angle and rate. The resulting pitch closed-loop becomes upon substitution of (6) into (4),

$$I_y\ddot{\theta} + k_{dp}\dot{\theta} + k_{pp}\theta = 0. \tag{7}$$

This is a standard second order system, and the gains k_{pp} and k_{dp} can be chosen in standard ways (see for example [24, sect. 5-3]. Most importantly, we have θ, $\dot{\theta} \to 0$ and $t \to \infty$.

To design the control law for the roll/yaw loop as well as the control law for momentum wheel management, we will consider the dynamics on the manifold $\theta = \dot{\theta} = 0$. We see from (6) that on this manifold, we have

$$\dot{h}_w = \tau_{c,y}. \tag{8}$$

Now, we have a constant desired set point for the wheel momentum $\bar{h}_w$ that we wish to maintain. We define the

error in wheel momentum as

$$\tilde{h}_w \triangleq h_w - \bar{h}_w. \tag{9}$$

The momentum wheel error dynamics therefore become

$$\dot{\tilde{h}}_w = \tau_{c,y}. \tag{10}$$

For small $\tilde{h}_w$, the roll/yaw and momentum wheel error equations can be written in linear time-invariant form

$$\begin{aligned} \dot{\mathbf{x}} &= \mathbf{A}\mathbf{x} + \mathbf{G}\boldsymbol{\tau}_c, \\ \dot{\tilde{h}}_w &= \mathbf{G}_w\boldsymbol{\tau}_c, \end{aligned} \tag{11}$$

where we have defined

$$\mathbf{x} = \begin{bmatrix} \phi \\ \psi \\ \dot{\phi} \\ \dot{\psi} \end{bmatrix}, \quad \mathbf{A} = \begin{bmatrix} 0 & 0 & 1 & 0 \\ 0 & 0 & 0 & 1 \\ 0 & 0 & 0 & \frac{\bar{h}_w}{I_x} \\ 0 & 0 & -\frac{\bar{h}_w}{I_z} & 0 \end{bmatrix}, \quad \mathbf{G} = \begin{bmatrix} 0 & 0 & 0 \\ 0 & 0 & 0 \\ \frac{1}{I_x} & 0 & 0 \\ 0 & 0 & \frac{1}{I_z} \end{bmatrix}, \quad \mathbf{G}_w = \begin{bmatrix} 0 & 1 & 0 \end{bmatrix}.$$

To perform the control system design and stability analysis, a transformation of variables will be useful. It can be verified by direct multiplication, that the transformation

$$\mathbf{T} = \begin{bmatrix} 1 & 0 & 0 & \frac{I_z}{\bar{h}_w} \\ 0 & 1 & -\frac{I_x}{\bar{h}_w} & 0 \\ 0 & 0 & \frac{1}{\sqrt{I_z}} & 0 \\ 0 & 0 & 0 & \frac{1}{\sqrt{I_x}} \end{bmatrix}, \tag{12}$$

has inverse

$$\mathbf{T}^{-1} = \begin{bmatrix} 1 & 0 & 0 & -\frac{I_z\sqrt{I_x}}{\bar{h}_w} \\ 0 & 1 & \frac{I_x\sqrt{I_z}}{\bar{h}_w} & 0 \\ 0 & 0 & \sqrt{I_z} & 0 \\ 0 & 0 & 0 & \sqrt{I_x} \end{bmatrix},$$

and that the transformation

$$\bar{\mathbf{A}} = \mathbf{T}\mathbf{A}\mathbf{T}^{-1} \tag{13}$$

results in

$$\bar{\mathbf{A}} = \begin{bmatrix} 0 & 0 & 0 & 0 \\ 0 & 0 & 0 & 0 \\ 0 & 0 & 0 & \frac{\bar{h}_w}{\sqrt{I_x I_z}} \\ 0 & 0 & -\frac{\bar{h}_w}{\sqrt{I_x I_z}} & 0 \end{bmatrix}. \tag{14}$$

We therefore make the transformation of variables

$$\bar{\mathbf{x}} = \mathbf{T}\mathbf{x}, \tag{15}$$

such that the roll/yaw and wheel error equations become

$$\begin{aligned} \dot{\bar{\mathbf{x}}} &= \bar{\mathbf{A}}\bar{\mathbf{x}} + \mathbf{T}\mathbf{G}\boldsymbol{\tau}_c, \\ \dot{\tilde{h}}_w &= \mathbf{G}_w \boldsymbol{\tau}_c. \end{aligned} \tag{16}$$

For the control system design, we now consider the Lyapunov-like function

$$V(\bar{\mathbf{x}}, \tilde{h}_w) = \frac{1}{2}\bar{\mathbf{x}}^T \mathbf{P}\bar{\mathbf{x}} + \frac{1}{2}k_w \tilde{h}_w^2, \tag{17}$$

where

$$\mathbf{P} = \begin{bmatrix} 1 & 0 & 0 & 0 \\ 0 & 1 & 0 & 0 \\ 0 & 0 & \bar{k} & 0 \\ 0 & 0 & 0 & \bar{k} \end{bmatrix}, \ \bar{k} > 0, \ \ k_w > 0.$$

It can readily be shown that $\bar{\mathbf{x}}^T \mathbf{P}\bar{\mathbf{A}}\bar{\mathbf{x}} = \mathbf{0}$. Therefore, taking the time-derivative of (17) along a trajectory of (16), we obtain

$$\dot{V} = \left[\bar{\mathbf{x}}^T \mathbf{P}\mathbf{T}\mathbf{G} + k_w \tilde{h}_w \mathbf{G}_w\right] \boldsymbol{\tau}_c. \tag{18}$$

Full three-axis torque

First, let us consider the situation when we have full availability of a three-axis torque, without any limitations. Let us choose the feedback control law

$$\boldsymbol{\tau}_c(\bar{\mathbf{x}}, \tilde{h}_w) = -K\left[k_w \tilde{h}_w \mathbf{G}_w^T + \mathbf{G}^T \mathbf{T}^T \mathbf{P}\bar{\mathbf{x}}\right], \ \ K > 0. \tag{19}$$

Then, we have

$$\dot{V} = -\frac{1}{K}\boldsymbol{\tau}_c^T \boldsymbol{\tau}_c \leq 0. \tag{20}$$

From this, we can conclude that $V(\bar{\mathbf{x}}(t), \tilde{h}_w(t)) \leq V(\bar{\mathbf{x}}(0), \tilde{h}_w(0))$ for all $t \geq 0$. Therefore, $\bar{\mathbf{x}}(t)$ and $\tilde{h}_w(t)$ are bounded. Hence, by its definition in (19), $\boldsymbol{\tau}_c(t)$ is bounded also. From (16), we now find that $\dot{\bar{\mathbf{x}}}$ and $\dot{\tilde{h}}_w$ are bounded also. Therefore, $\bar{\mathbf{x}}(t)$ and $\tilde{h}_w(t)$, and consequently $\boldsymbol{\tau}_c$ are bounded uniformly continuous functions of time. Consequently, from (20), we find that $\dot{V}(t)$ is a uniformly continuous function of time. Since $V(t) \geq 0$ and $\dot{V} \leq 0$, the integral $\int_0^t \dot{V} dt$ is non-increasing and bounded below by $-V(0)$. Therefore, the integral $\int_0^\infty \dot{V} dt$ exists and is finite. From Barbalat's lemma [25, p. 192], we have that $\dot{V} \to 0$ as $t \to \infty$ and consequently from (20), $\boldsymbol{\tau}_c \to \mathbf{0}$ as $t \to \infty$. Since $(\bar{\mathbf{x}}(t), \tilde{h}_w(t))$ is contained in the compact set $\{(\mathbf{y}, z) \in R^4 \times R : V(\mathbf{y}, z) \leq V(\bar{\mathbf{x}}(0), \tilde{h}_w(0))\}$ for all $t \geq 0$, and since $\boldsymbol{\tau}_c(\mathbf{y}, z)$ is clearly continuous, we have from Proposition 1 that $(\bar{\mathbf{x}}(t), \tilde{h}_w(t))$ approaches the set $G \triangleq \{(\mathbf{y}, z) \in R^4 \times R : \boldsymbol{\tau}_c(\mathbf{y}, z) = \mathbf{0}\}$ as $t \to \infty$.

With the control law given by (19), when applied to (16) the closed-loop equations are autonomous. Therefore, the positive limit set of every closed-loop trajectory is invariant under the closed-loop dynamics, and since all trajectories $\bar{\mathbf{x}}(t)$ and $\tilde{h}_w(t)$ are bounded, they must approach their positive limit sets [25, p. 114]. As such, every closed-loop trajectory approaches the largest invariant set contained in G. Setting $\boldsymbol{\tau}_c = \mathbf{0}$ in (16), we see that every invariant set contained in G must contain a trajectory of the open-loop system,

$$\begin{aligned} \dot{\bar{\mathbf{x}}} &= \bar{\mathbf{A}}\bar{\mathbf{x}}, \\ \dot{\tilde{h}}_w &= 0, \end{aligned} \tag{21}$$

satisfying $\boldsymbol{\tau}_c(\bar{\mathbf{x}}, \tilde{h}) = \mathbf{0}$. We can readily find that the solutions of the open-loop system are given by

$$\begin{aligned} \bar{x}_1(t) &= \bar{x}_1(0), \\ \bar{x}_2(t) &= \bar{x}_2(0), \\ \bar{x}_3(t) &= \bar{x}_3(0)\cos bt + \bar{x}_4(0)\sin bt, \\ \bar{x}_4(t) &= -\bar{x}_3(0)\sin bt + \bar{x}_4(0)\cos bt, \\ \tilde{h}(t) &= \tilde{h}(0), \end{aligned} \tag{22}$$

where $b = \frac{\bar{h}_w}{\sqrt{I_x I_z}}$. Now, let the set F be any invariant set under (21). We now see that if $(\mathbf{y}, z) \in F$, then it must be that $(\bar{\mathbf{y}}(s), \bar{z}(s)) \in F$ for all $0 \leq s \leq \frac{2\pi}{b}$, where

$$\bar{\mathbf{y}}(s) = \begin{bmatrix} y_1 \\ y_2 \\ y_3 \cos bs + y_4 \sin bs \\ -y_3 \sin bs + y_4 \cos bs \end{bmatrix}, \quad \bar{z}(s) = z.$$

Now, let E be any invariant set satisfying $E \subset G$, and let $(\mathbf{y}, z) \in E$. Then, upon expanding (19) we see that this is

only possible if

$$\begin{aligned} \tfrac{K}{h_w} y_2 - \tfrac{K\bar{k}}{I_x\sqrt{I_z}} \left[y_3 \cos bs + y_4 \sin bs \right] &= 0, \\ -K k_w z &= 0, \\ -\tfrac{K}{h_w} y_1 - \tfrac{K\bar{k}}{I_z\sqrt{I_x}} \left[-y_3 \sin bs + y_4 \cos bs \right] &= 0, \end{aligned}$$

for all $0 \leq s \leq \frac{2\pi}{b}$. Clearly, this is possible only if $(\mathbf{y}, z) = (\mathbf{0}, 0)$. That is, the largest invariant set $E \subset G$ is $E = \{(\mathbf{0}, 0)\}$. Therefore, we can conclude that all trajectories of the closed-loop system satisfy $\bar{\mathbf{x}}(t) \to \mathbf{0}$ and $\tilde{h}_w(t) \to 0$ as $t \to \infty$.

Let us now examine the control law in terms of the original state vector, $\mathbf{x}$. Substituting (15) into (19), and expanding, we find that

$$\boldsymbol{\tau}_c = \begin{bmatrix} \frac{K}{h_w}\psi - K\left(\frac{I_x}{h_w^2} + \frac{\bar{k}}{I_x I_z}\right)\dot{\phi} \\ -K k_w \tilde{h}_w \\ -\frac{K}{h_w}\phi - K\left(\frac{I_z}{h_w^2} + \frac{\bar{k}}{I_x I_z}\right)\dot{\psi} \end{bmatrix}. \tag{23}$$

Now, let us define $\bar{K} = \frac{K}{h_w}$, $\bar{k}' = \frac{\bar{k}\bar{h}_w}{I_x I_z}$ and $k'_w = K k_w$. Then, we can rewrite the control law (23) as

$$\boldsymbol{\tau}_c = \begin{bmatrix} \bar{K}\psi - \bar{K}\left(\frac{I_x}{h_w} + \bar{k}'\right)\dot{\phi} \\ -k'_w \tilde{h}_w \\ -\bar{K}\phi - \bar{K}\left(\frac{I_z}{h_w} + \bar{k}'\right)\dot{\psi} \end{bmatrix}. \tag{24}$$

To summarize, we obtain the following theorem.

Theorem 2

Consider the feedback control law (24), with $k'_w > 0$ and $\text{sign}[\bar{K}] = \text{sign}[\bar{k}'] = \text{sign}[\bar{h}_w]$ with $\bar{K} \neq 0$ and $\bar{k}' \neq 0$. Then, when applied to the roll/yaw and wheel error system (11), the closed-loop system is stable and $\mathbf{x} \to \mathbf{0}$, $\tilde{h}_w \to 0$ as $t \to \infty$.

Magnetic actuation with saturation constraints

Let us now examine the implementation of the control law (24) when using magnetic actuation under saturation constraints.

The control torque provided by a magnetic torquer is given by [2, p. 636]

$$\boldsymbol{\tau}_c = -\mathbf{B}^{\times}\mathbf{W}\mathbf{m}, \tag{25}$$

where $\mathbf{B}$ is the Earth's magnetic field expressed in spacecraft body coordinates, and $\mathbf{m}$ is the magnetic torquer dipole moment (expressed in spacecraft body coordinates). The matrix $\mathbf{W}$ is defined to select active magnetic torque rods,

and is defined as

$$\mathbf{W} \triangleq \text{diag}\left(W_x, W_y, W_z\right), \;\; W_i = \begin{cases} 1, & i\text{th torquer available,} \\ 0, & i\text{th torquer not available.} \end{cases}, \;\; i = x, y, z. \tag{26}$$

For example, if only magnetic torque rods aligned with the body x- and y- axes are available, then $\mathbf{W} = \text{diag}\left(1, 1, 0\right)$. We now impose the following magnetic torquer limitations

$$-\mathbf{m}_{max} \leq \mathbf{m} \leq \mathbf{m}_{max}, \;\; \mathbf{m}_{max} > \mathbf{0} \tag{27}$$

where $\mathbf{m}_{max}$ is a vector of maximum dipole moments about each axis, and the inequalities in (27) are taken componentwise.

Choosing the same Lyapunov-like function (17), its time derivative along a trajectory of (16) with magnetic actuation (25) becomes

$$\dot{V} = \mathbf{F}^T(\bar{\mathbf{x}}, \tilde{h}_w, t)\mathbf{m}, \tag{28}$$

where we have defined

$$\mathbf{F}(\mathbf{a}, b, t) = \mathbf{W}\mathbf{B}(t)^{\times}\left[k_w b \mathbf{G}_w^T + \mathbf{G}^T\mathbf{T}^T\mathbf{P}\mathbf{a}\right]. \tag{29}$$

We now choose the control law to be

$$\mathbf{m} = \text{sat}\left[-\frac{K}{||\mathbf{B}||^2}\mathbf{F}(\bar{\mathbf{x}}, \tilde{h}_w, t), \mathbf{m}_{max}\right], \tag{30}$$

where $K > 0$, and the saturation function is defined componentwise by

$$\left\{\text{sat}\left[\mathbf{x}, \mathbf{x}_{max}\right]\right\}_i = \begin{cases} \{\mathbf{x}\}_i, & |\{\mathbf{x}\}_i| \leq \{\mathbf{x}_{max}\}_i, \\ \{\mathbf{x}_{max}\}_i \text{sign}\left[\{\mathbf{x}\}_i\right], & |\{\mathbf{x}\}_i| > \{\mathbf{x}_{max}\}_i. \end{cases} \quad i = x, y, z. \tag{31}$$

We then find that

$$\dot{V} = -\left[f\left(\{\mathbf{F}\}_x, \{\mathbf{m}_{max}\}_x\right) + f\left(\{\mathbf{F}\}_y, \{\mathbf{m}_{max}\}_y\right) + f\left(\{\mathbf{F}\}_z, \{\mathbf{m}_{max}\}_z\right)\right]. \tag{32}$$

where we have defined the function

$$f(x, x_{max}) = \begin{cases} \frac{Kx^2}{||\mathbf{B}||^2}, & \frac{K|x|}{||\mathbf{B}||^2} \leq x_{max}, \\ |x|x_{max}, & \frac{K|x|}{||\mathbf{B}||^2} > x_{max}. \end{cases} \tag{33}$$

with $x_{max} > 0$. Clearly, $f(x, x_{max}) \geq 0$, and $f(x, x_{max}) = 0$ if and only if $x = 0$. Returning to (32), we again find

that $V(\bar{\mathbf{x}}(t), \tilde{h}_w(t)) \leq V(\bar{\mathbf{x}}(0), \tilde{h}_w(0))$ for all $t \geq 0$. Therefore, $\bar{\mathbf{x}}(t)$ and $\tilde{h}_w(t)$ are bounded. Clearly, by its definition (30), $\mathbf{m}$ is bounded. We now make the following assumption on the Earth's magnetic field.

Assumption 1

It is assumed that $\mathbf{B}$ is a uniformly continuous function of time, and that there exist $B_{min} > 0$ and $B_{max} > 0$ such that $B_{min} \leq ||\mathbf{B}|| \leq B_{max}$.

Making use of Assumption 1, we find from (25) that $\boldsymbol{\tau}_c$ is bounded, and hence from (16), that $\dot{\bar{\mathbf{x}}}$ and $\dot{\tilde{h}}_w$ are bounded also. Therefore, $\bar{\mathbf{x}}(t)$ and $\tilde{h}_w(t)$ and are bounded uniformly continuous functions of time. Making use of this fact, and Assumption 1, we find that $\mathbf{F}(\bar{\mathbf{x}}, \tilde{h}_w, t)$ and $\frac{K}{||\mathbf{B}||^2}\mathbf{F}(\bar{\mathbf{x}}, \tilde{h}_w, t)$ are bounded uniformly continuous functions of time. Now, it can be readily verified that the saturation function (31) is uniformly continuous in $\mathbf{x}$. Therefore, from (30) we find that $\mathbf{m}$ is bounded and uniformly continuous in time. Finally, from (28) we find that $\dot{V}$ is uniformly continuous in time. Since $V(t) \geq 0$ and $\dot{V} \leq 0$, the integral $\int_0^t \dot{V} dt$ is non-increasing and bounded below by $-V(0)$. Therefore, the integral $\int_0^\infty \dot{V} dt$ exists and is finite. From Barbalat's lemma [25, p. 192], we have that $\dot{V} \to 0$ as $t \to \infty$. From (32), we see that this implies $\mathbf{F}(\bar{\mathbf{x}}, \tilde{h}_w, t) \to \mathbf{0}$ and consequently from (30) that $\mathbf{m}$ as $t \to \infty$. Finally, since $\mathbf{B}$ is bounded by Assumption 1, (25) shows that $\boldsymbol{\tau}_c \to \mathbf{0}$ as $t \to \infty$.

We now make another assumption on the Earth's magnetic field.

Assumption 2

Let $\mathbf{f}$, $\mathbf{g}$, $\mathbf{h} \in R^3$. Assume that at least one of $\mathbf{f}$, $\mathbf{g}$ or $\mathbf{h}$ is non-zero. Let $b \neq 0$ be given. Then, $\exists \epsilon > 0,\ T > 0$, such that $\forall t \geq 0$ there exists t' contained in the interval $[0, T]$ for which

$$\left|\mathbf{B}(t+t')^T \left[\mathbf{f} + \mathbf{g}\sin bt' + \mathbf{h}\cos bt'\right]\right| > \epsilon.$$

Remark

Assumption 2 (and later Assumption 2') can be thought of as a type of controllability condition. Physically, it means that the Earth's magnetic field is "rich enough" for the orbit under consideration. The implication of Assumption 2 (and later Assumption 2'), is that there is no natural (unforced) spacecraft attitude motion with non-zero attitude error such that the feedback control input vanishes. Given the various anomalies in the Earth's magnetic field (see [2, sect. 5.1]), both Assumptions 2 and 2' are very reasonable for orbits with non-zero inclination.

Now, let $\left(\bar{\mathbf{x}}(t), \tilde{h}_w(t)\right)$ be a solution of the closed-loop system

$$\begin{aligned} \dot{\bar{\mathbf{x}}} &= \bar{\mathbf{A}}\bar{\mathbf{x}} + \mathbf{TG}\boldsymbol{\tau}_c(\bar{\mathbf{x}}, \tilde{h}_w, t), \quad \bar{\mathbf{x}}(0) = \bar{\mathbf{x}}_0, \\ \dot{\tilde{h}}_w &= \mathbf{G}_w\boldsymbol{\tau}_c, \qquad\qquad\qquad\qquad \tilde{h}_w(0) = \tilde{h}_{w0}. \end{aligned} \tag{34}$$

where

$$\boldsymbol{\tau}_c(\bar{\mathbf{x}}, \tilde{h}_w, t) = -\mathbf{B}^{\times}\mathbf{W}\mathbf{m}(\bar{\mathbf{x}}, \tilde{h}_w, t),$$

and $\mathbf{m}(\bar{\mathbf{x}}, \tilde{h}_w, t)$ is given by (30). Then, $\left(\bar{\mathbf{x}}(t), \tilde{h}_w(t)\right)$ is also a solution of

$$\begin{aligned} \dot{\mathbf{y}} &= \bar{\mathbf{A}}\mathbf{y} + \mathbf{p}(t), \quad \mathbf{y}(0) = \bar{\mathbf{x}}_0, \\ \dot{z} &= q(t), \qquad\qquad z(0) = \tilde{h}_{w0}, \end{aligned} \tag{35}$$

where

$$\mathbf{p}(t) = \mathbf{TG}\boldsymbol{\tau}_c(\bar{\mathbf{x}}(t), \tilde{h}_w(t), t), \;\; q(t) = \mathbf{G}_w\boldsymbol{\tau}_c(\bar{\mathbf{x}}(t), \tilde{h}_w(t), t).$$

From our previous analysis, we find that $\mathbf{p}(t) \to 0$ and $q(t) \to 0$ as $t \to \infty$. Therefore, $\bar{\mathbf{A}}\mathbf{y} + \mathbf{p}(t) \to \bar{\mathbf{A}}\mathbf{y}$ uniformly in $\mathbf{y}$ as $t \to \infty$. Since $\left(\bar{\mathbf{x}}(t), \tilde{h}_w(t)\right)$ is contained in the compact set $\{(\mathbf{y}, z) \in R^4 \times R : V(\mathbf{y}, z) \leq V(\bar{\mathbf{x}}(0), \tilde{h}_w(0))\}$ for all $t \geq 0$, Theorem 1 now tells us that for any sequence $t_m \to \infty$, there exists a subsequence t_{mj} and a solution $(\mathbf{y}(t), z(t))$ of

$$\begin{aligned} \dot{\mathbf{y}} &= \bar{\mathbf{A}}\mathbf{y}, \\ \dot{z} &= 0, \end{aligned} \tag{36}$$

such that $\left(\bar{\mathbf{x}}(t + t_{mj}), \tilde{h}_w(t + t_{mj})\right) \to (\mathbf{y}(t), z(t))$ as $mj \to \infty$ uniformly in t on compact subsets of R. As we have already seen in (22), $\mathbf{y}(t)$ and $z(t)$ have the form

$$\begin{aligned} y_1(t) &= y_{10}, \\ y_2(t) &= y_{20}, \\ y_3(t) &= y_{30}\cos bt + y_{40}\sin bt, \\ y_4(t) &= -y_{30}\sin bt + y_{40}\cos bt, \\ z(t) &= z_0, \end{aligned} \tag{37}$$

We know that $\mathbf{F}(\bar{\mathbf{x}}(t), \tilde{h}_w(t), t) \to \mathbf{0}$ as $t \to \infty$. Let us now examine the implications of this on $(\mathbf{y}(t), z(t))$. First, we note that since $\mathbf{B}$ is bounded (by Assumption 1), and since $\mathbf{F}(\mathbf{a}, b, t)$ is linear in $(\mathbf{a}, b)$ (as can be seen in (29)), $\mathbf{F}(\mathbf{a}, b, t)$ is Lipschitz continuous in $(\mathbf{a}, b)$ on $R^4 \times R$ uniformly in t, which means that it is uniformly continuous in $(\mathbf{a}, b)$ on $R^4 \times R$ uniformly in t.

Now, let us find $\mathbf{F}\left(\mathbf{y}(t), z(t), t+t_{mj}\right)$. Substituting (37) into (29), we find that

$$\mathbf{F}\left(\mathbf{y}(t), z(t), t+t_{mj}\right) = \begin{bmatrix} F_x\left(\mathbf{y}(t), z(t), t+t_{mj}\right) \\ F_y\left(\mathbf{y}(t), z(t), t+t_{mj}\right) \\ F_z\left(\mathbf{y}(t), z(t), t+t_{mj}\right) \end{bmatrix},$$

where

$$F_x\left(\mathbf{y}(t), z(t), t+t_{mj}\right) = W_x \mathbf{B}^T(t+t_{mj}) \left(\begin{bmatrix} 0 \\ \frac{y_{10}}{h_w} \\ -k_w z_0 \end{bmatrix} + \begin{bmatrix} 0 \\ -\frac{\bar{k} y_{30}}{I_z\sqrt{I_x}} \\ 0 \end{bmatrix} \sin bt + \begin{bmatrix} 0 \\ \frac{\bar{k} y_{40}}{I_z\sqrt{I_x}} \\ 0 \end{bmatrix} \cos bt \right), \tag{38}$$

$$F_y\left(\mathbf{y}(t), z(t), t+t_{mj}\right) = W_y \mathbf{B}^T(t+t_{mj}) \left(\begin{bmatrix} -\frac{y_{10}}{h_w} \\ 0 \\ -\frac{y_{20}}{h_w} \end{bmatrix} + \begin{bmatrix} \frac{\bar{k} y_{30}}{I_z\sqrt{I_x}} \\ 0 \\ \frac{\bar{k} y_{40}}{I_x\sqrt{I_z}} \end{bmatrix} \sin bt + \begin{bmatrix} -\frac{\bar{k} y_{40}}{I_z\sqrt{I_x}} \\ 0 \\ \frac{\bar{k} y_{30}}{I_x\sqrt{I_z}} \end{bmatrix} \cos bt \right), \tag{39}$$

$$F_z\left(\mathbf{y}(t), z(t), t+t_{mj}\right) = W_z \mathbf{B}^T(t+t_{mj}) \left(\begin{bmatrix} k_w z_0 \\ \frac{y_{20}}{h_w} \\ 0 \end{bmatrix} + \begin{bmatrix} 0 \\ -\frac{\bar{k} y_{40}}{I_x\sqrt{I_z}} \\ 0 \end{bmatrix} \sin bt + \begin{bmatrix} 0 \\ -\frac{\bar{k} y_{30}}{I_x\sqrt{I_z}} \\ 0 \end{bmatrix} \cos bt \right). \tag{40}$$

Let us assume that $(\mathbf{y}(t), z(t))$ is non-zero, that is at least one of y_{10}, y_{20}, y_{30}, y_{40}, and z_0 in (37) is non-zero. Let there be at least two available magnetic torquers (at least two of W_x, W_y, and W_z are equal to 1). Then, the non-zero terms in $\{y_{10}, y_{20}, y_{30}, y_{40}, z_0\}$ appear in at least one F_i with $W_i = 1$ for $i \in \{x, y, z\}$. By Assumption 2, there exists an $\epsilon' > 0$, $T > 0$ and $t'_{mj} \in [0, T]$ such that $|F_i\left(\mathbf{y}(t'_{mj}), z(t'_{mj}), t'_{mj} + t_{mj}\right)| > \epsilon'$, for all t_{mj}. Therefore, there exists an $\epsilon > \epsilon' > 0$ such that $||\mathbf{F}\left(\mathbf{y}(t'_{mj}), z(t'_{mj}), t'_{mj} + t_{mj}\right)|| > \epsilon$ for all t_{mj}.

By uniform continuity of $\mathbf{F}(\mathbf{a}, b, t)$, there exists a $\delta > 0$ such that if $||(\mathbf{a}, b) - \left(\mathbf{y}(t'_{mj}), z(t'_{mj})\right)|| < \delta$, then $||\mathbf{F}\left(\mathbf{a}, b, t'_{mj} + t_{mj}\right)|| > \frac{\epsilon}{2}$. Now, since $\left(\bar{\mathbf{x}}(t+t_{mj}), \tilde{h}_w(t+t_{mj})\right) \to (\mathbf{y}(t), z(t))$ as $mj \to \infty$ uniformly in t on $t \in [0, T]$, there exists an integer $N \geq 0$ such that $||\left(\bar{\mathbf{x}}(t+t_{mj}), \tilde{h}_w(t+t_{mj})\right) - (\mathbf{y}(t), z(t))|| < \delta$ for all $t \in [0, T]$ and $mj \geq N$. In particular, this implies that for all $mj \geq N$, $||\mathbf{F}\left(\bar{\mathbf{x}}(t'_{mj}+t_{mj}), \tilde{h}_w(t'_{mj}+t_{mj}), t'_{mj}+t_{mj}\right)|| > \frac{\epsilon}{2}$. This contradicts the convergence of $\mathbf{F}(\bar{\mathbf{x}}(t), \tilde{h}_w(t), t) \to \mathbf{0}$ as $t \to \infty$. Therefore, we must have $(\mathbf{y}(t), z(t)) \equiv (\mathbf{0}, 0)$, and we see that $\left(\bar{\mathbf{x}}(t+t_{mj}), \tilde{h}_w(t+t_{mj})\right) \to (\mathbf{0}, 0)$ as $mj \to \infty$. Therefore, $(\mathbf{0}, 0)$ is contained in the positive limit set of $\left(\bar{\mathbf{x}}(t), \tilde{h}_w(t)\right)$. In fact, since Theorem 1 holds for any sequence $t_m \to \infty$, this shows that the positive limit set of $\left(\bar{\mathbf{x}}(t), \tilde{h}_w(t)\right)$ is equal to $\{(\mathbf{0}, 0)\}$. Since $\left(\bar{\mathbf{x}}(t), \tilde{h}_w(t)\right)$ is bounded, it must approach its positive limit set at $t \to \infty$ [25, p. 114]. We can therefore conclude that $\left(\bar{\mathbf{x}}(t), \tilde{h}_w(t)\right) \to (\mathbf{0}, 0)$ as $t \to \infty$.

Let us now examine the control law (30) in terms of the original state vector x. We find after some manipulations

that the control law can be written as

$$\mathbf{m} = \text{sat}\left[\frac{\mathbf{W}\mathbf{B}^{\times}\boldsymbol{\tau}_{cd}}{||\mathbf{B}||^2}, \mathbf{m}_{max}\right], \tag{41}$$

where

$$\boldsymbol{\tau}_{cd} = \begin{bmatrix} \bar{K}\psi - \bar{K}\left(\frac{I_x}{\bar{h}_w} + \bar{k}'\right)\dot{\phi} \\ -k'_w\tilde{h}_w \\ -\bar{K}\phi - \bar{K}\left(\frac{I_z}{\bar{h}_w} + \bar{k}'\right)\dot{\psi} \end{bmatrix},$$

represents the desired (ideal) control torque as in (24), and $\bar{K} = \frac{K}{\bar{h}_w}$, $\bar{k}' = \frac{\bar{k}\bar{h}_w}{I_x I_z}$ and $k'_w = Kk_w$.

To summarize, we obtain the following theorem.

Theorem 3

Let Assumptions 1 and 2 hold, and let at least two of W_x, W_y and W_z be non-zero. Consider the feedback control law (41), with $k'_w > 0$ and $\text{sign}[\bar{K}] = \text{sign}[\bar{k}'] = \text{sign}[\bar{h}_w]$ with $\bar{K} \neq 0$ and $\bar{k}' \neq 0$. Then, when applied to the roll/yaw and wheel error system (11) with (25), the closed-loop system is stable and $\mathbf{x} \to \mathbf{0}$, $\tilde{h}_w \to 0$ as $t \to \infty$.

4.2 Bias-Momentum Spacecraft

As for the dual-spin case, it is clear from (5) that the roll and yaw equations can be decoupled from the pitch equation. We make use of the dual-spin pitch control law (6) with the added restriction that $k_{pp} + 3(I_x - I_z)\omega_o^2 > 0$. As a result, we have θ, $\dot{\theta} \to 0$ and $t \to \infty$.

As in the dual-spin case, we will consider the dynamics on the manifold $\theta = \dot{\theta} = 0$ for the purpose of roll/yaw loop and momentum wheel management control design. As in the dual-spin case, we have a constant desired set point for the wheel momentum $\bar{h}_w$ that we wish to maintain, and on the manifold $\theta = \dot{\theta} = 0$, the wheel error dynamics are given by (10).

For small $\tilde{h}_w$, the roll/yaw and momentum wheel error equations can be written in linear time-invariant form (11), where the definitions of $\mathbf{x}$, $\mathbf{G}$ and $\mathbf{G}_w$ are the same as in the dual-spin case, but $\mathbf{A}$ is replaced with

$$\mathbf{A} = \begin{bmatrix} 0 & 0 & 1 & 0 \\ 0 & 0 & 0 & 1 \\ \frac{b}{I_x} & 0 & 0 & \frac{a}{I_x} \\ 0 & \frac{c}{I_z} & -\frac{a}{I_z} & 0 \end{bmatrix}, \tag{42}$$

where

$$a = (I_x + I_z - I_y)\omega_o + \bar{h}_w, \;\; b = \omega_o\bar{h}_w - 4(I_y - I_z)\omega_o^2, \;\; c = \omega_o\bar{h}_w - (I_y - I_x)\omega_o^2.$$

It will be assumed that the bias momentum $\bar{h}_w$ will be chosen such that the bias momentum spacecraft is open-loop stable (otherwise it does not make sense as a bias momentum spacecraft). In this case, it can readily be shown that

$\mathbf{A}$ in (42) has eigenvalues

$$\lambda = \pm jm_1, \pm jm_2, \tag{43}$$

where

$$m_1 = \left(\frac{a^2 - I_x c - I_z b - \sqrt{(a^2 - I_x c - I_z b)^2 - 4bcI_x I_z}}{2I_x I_z} \right)^{\frac{1}{2}}, \tag{44}$$

$$m_2 = \left(\frac{a^2 - I_x c - I_z b + \sqrt{(a^2 - I_x c - I_z b)^2 - 4bcI_x I_z}}{2I_x I_z} \right)^{\frac{1}{2}}. \tag{45}$$

Clearly then, $\mathbf{A}$ in (42) has the same eigenvalues as

$$\bar{\mathbf{A}} = \begin{bmatrix} 0 & m_1 & 0 & 0 \\ -m_1 & 0 & 0 & 0 \\ 0 & 0 & 0 & m_2 \\ 0 & 0 & -m_2 & 0 \end{bmatrix}. \tag{46}$$

As in the dual-spin case, to perform the control system design and stability analysis, a transformation of variables will be useful. In particular, we seek a transformation $\mathbf{T}$ such that $\bar{\mathbf{A}} = \mathbf{TAT}^{-1}$. To this end, let $\mathbf{E}_A$ and $\mathbf{E}_{\bar{A}}$ be matrices such that

$$\mathbf{AE}_A = \mathbf{E}_A \mathbf{\Lambda}, \;\; \bar{\mathbf{A}}\mathbf{E}_{\bar{A}} = \mathbf{E}_{\bar{A}} \mathbf{\Lambda},$$

where $\mathbf{\Lambda} = \text{diag}(jm_1, -jm_1, jm_2, -jm_2)$. Since the eigenvalues of $\mathbf{A}$ and $\bar{\mathbf{A}}$ are distinct, both $\mathbf{E}_A$ and $\mathbf{E}_{\bar{A}}$ are invertible, and a transformation $\mathbf{T}$ that satisfies $\bar{\mathbf{A}} = \mathbf{TAT}^{-1}$ is given by $\mathbf{T} = \mathbf{E}_{\bar{A}} \mathbf{E}_A^{-1}$.

Assuming that $a \neq 0$, it is straightforward to show that the matrices

$$\mathbf{E}_{\bar{A}} = \begin{bmatrix} 1 & 1 & 0 & 0 \\ j & -j & 0 & 0 \\ 0 & 0 & 1 & 1 \\ 0 & 0 & j & -j \end{bmatrix},$$

and

$$\mathbf{E}_A = \begin{bmatrix} g & g & h & h \\ j\left(\frac{b+I_x m_1^2}{am_1}\right) g & -j\left(\frac{b+I_x m_1^2}{am_1}\right) g & j\left(\frac{b+I_x m_2^2}{am_1}\right) h & -j\left(\frac{b+I_x m_2^2}{am_1}\right) h \\ jm_1 g & -jm_1 g & jm_2 h & -jm_2 h \\ -\left(\frac{b+I_x m_1^2}{a}\right) g & -\left(\frac{b+I_x m_1^2}{a}\right) g & -\left(\frac{b+I_x m_2^2}{a}\right) h & -\left(\frac{b+I_x m_2^2}{a}\right) h \end{bmatrix}, \;\; g, h \neq 0,$$

have the required properties. After some tedious algebra, the sought after transformation can be found as

$$\mathbf{T} = \begin{bmatrix} \frac{b+I_x m_2^2}{gI_x(m_2^2-m_1^2)} & 0 & 0 & \frac{a}{gI_x(m_2^2-m_1^2)} \\ 0 & \frac{am_1m_2^2}{gb(m_2^2-m_1^2)} & -\frac{m_1(b+I_x m_2^2)}{gb(m_2^2-m_1^2)} & 0 \\ -\frac{b+I_x m_1^2}{hI_x(m_2^2-m_1^2)} & 0 & 0 & -\frac{a}{hI_x(m_2^2-m_1^2)} \\ 0 & \frac{am_1^2m_2}{hb(m_2^2-m_1^2)} & -\frac{m_2(b+I_x m_1^2)}{hb(m_2^2-m_1^2)} & 0 \end{bmatrix}, \quad g, h \neq 0. \tag{47}$$

As in the dual-spin case, we make the transformation of variables given in (15), where $\mathbf{T}$ is replaced with (47). Then, the roll/yaw and wheel error equations obtain the same form as in the dual-spin case, given by (16), where $\bar{\mathbf{A}}$ is replaced with (46) (and $\mathbf{T}$ is replaced with (47)).

For the control system design, we make use of the same Lyapunov-like function as in the dual-spin case (17). As in the dual-spin case, $\bar{\mathbf{x}}^T\mathbf{P}\bar{\mathbf{A}}\bar{\mathbf{x}} = \mathbf{0}$ and the time-derivative of (17) along a trajectory of (16) (with $\mathbf{A}$ and $\mathbf{T}$ replaced by (46) and (47) respectively) is given by (18) (with $\mathbf{T}$ replaced by (47)).

Full three-axis torque

As in the dual-spin case, we first consider the situation when we have full availability of a three-axis torque, without any limitations. We choose a feedback control law of the same form as in the dual-spin case, namely

$$\boldsymbol{\tau}_c(\bar{\mathbf{x}}, \tilde{h}_w) = -K\left[k_w\tilde{h}_w\mathbf{G}_w^T + \mathbf{G}^T\mathbf{T}^T\mathbf{P}\bar{\mathbf{x}}\right], \quad K > 0, \tag{48}$$

where $\mathbf{T}$ is given by (47).

It is easy to show that the solutions of the open-loop system

$$\begin{aligned} \dot{\bar{\mathbf{x}}} &= \bar{\mathbf{A}}\bar{\mathbf{x}}, \\ \dot{\tilde{h}}_w &= 0, \end{aligned} \tag{49}$$

are given by

$$\begin{aligned} \bar{x}_1(t) &= \bar{x}_1(0)\cos m_1 t + \bar{x}_2(0)\sin m_1 t, \\ \bar{x}_2(t) &= -\bar{x}_1(0)\sin m_1 t + \bar{x}_2(0)\cos m_1 t, \\ \bar{x}_3(t) &= \bar{x}_3(0)\cos m_2 t + \bar{x}_4(0)\sin m_2 t, \\ \bar{x}_4(t) &= -\bar{x}_3(0)\sin m_2 t + \bar{x}_4(0)\cos m_2 t, \\ \tilde{h}(t) &= \tilde{h}(0), \end{aligned} \tag{50}$$

Expanding (49), we obtain

$$\boldsymbol{\tau}_c(\bar{\mathbf{x}},\tilde{h}_w)=\begin{bmatrix} \frac{Km_1(b+I_xm_2^2)}{gbI_x(m_2^2-m_1^2)}\bar{x}_2-\frac{K\bar{k}m_2(b+I_xm_2^1)}{hbI_x(m_2^2-m_1^2)}\bar{x}_4 \\ -Kk_w\tilde{h}_w \\ -\frac{a}{gI_xI_z(m_2^2-m_1^2)}\bar{x}_1+\frac{K\bar{k}a}{hI_xI_z(m_2^2-m_1^2)}\bar{x}_3 \end{bmatrix}. \tag{51}$$

From (50) and (51), it is found that the only open-loop solution contained in the set $G\triangleq\{(\mathbf{y},z)\in R^4\times R:\ \boldsymbol{\tau}_c(\mathbf{y},z)=\mathbf{0}\}$ as $t\to\infty$, is the trivial solution $(\bar{\mathbf{x}}(t),\tilde{h}_w(t))\equiv(\mathbf{0},0)$. Using this fact, all of the arguments in the dual-spin case can be repeated to conclude that all trajectories of the closed-loop system satisfy $\bar{\mathbf{x}}(t)\to\mathbf{0}$ and $\tilde{h}_w(t)\to 0$ as $t\to\infty$.

Let us now examine the control law in terms of the original state vector, $\mathbf{x}$. Substituting (15) with (47) into (48) and expanding, we find that

$$\boldsymbol{\tau}_c=\begin{bmatrix} k_{G\phi}\psi-k_{d\phi}\dot{\phi} \\ -k_w'\tilde{h}_w \\ -k_{G\psi}\phi-k_{d\psi}\dot{\psi} \end{bmatrix}, \tag{52}$$

where

$$\begin{aligned} k_{G\phi} &= \tfrac{Kac}{bI_x^2I_z(m_2^2-m_1^2)^2}\left(\tfrac{b+I_xm_2^2}{g^2}+\tfrac{\bar{k}(b+I_xm_1^2)}{h^2}\right) \\ k_{G\psi} &= \tfrac{b}{c}k_{G\phi} \\ k_{d\phi} &= \tfrac{K}{b^2I_x(m_2^2-m_1^2)^2}\left(\tfrac{m_1^2(b+I_xm_2^2)^2}{g^2}+\tfrac{\bar{k}m_2^2(b+I_xm_1^2)^2}{h^2}\right) \\ k_{d\psi} &= \tfrac{Ka^2}{I_x^2I_z(m_2^2-m_1^2)^2}\left(\tfrac{1}{g^2}+\tfrac{\bar{k}}{h^2}\right) \end{aligned} \tag{53}$$

In summary, we obtain the following theorem.

Theorem 4

Consider the feedback control law (52), with $K>0$ $\bar{k}>0$, $k_w'>0$, $g\neq 0$ and $h\neq 0$. Then, when applied to the bias momentum roll/yaw and wheel error system (11) with $\mathbf{A}$ given by (42), the closed-loop system is stable and $\mathbf{x}\to\mathbf{0}$, $\tilde{h}_w\to 0$ as $t\to\infty$.

Let us now obtain some further insight into the roll/yaw gains (53). First, from (53), we see that the derivative gains are positive, that is $k_{d\phi},k_{d\psi}>0$. Typically, for a bias-momentum satellite, $|\bar{h}_w|>>|I_x\omega_o|,|I_y\omega_o|,|I_z\omega_o|$. Making these approximations, and setting $g=\frac{\sqrt{I_x}}{\omega_o}$, $h=\frac{\sqrt{I_xI_z}}{|\bar{h}_w|}$, the gains in (53) become

$$\begin{aligned} k_{G\phi} &\approx k_{G\psi}\approx \tfrac{K\omega_o}{\bar{h}_wI_x}\left(\omega_o+\bar{k}\bar{h}_w\right), \\ k_{d\phi} &\approx \tfrac{KI_z}{\bar{h}_w^2}\left(\tfrac{\omega_o^2}{I_z}+\tfrac{\bar{k}\bar{h}_w^2}{I_xI_z}\right), \\ k_{d\psi} &\approx \tfrac{KI_z}{\bar{h}_w^2}\left(\tfrac{\omega_o^2}{I_x}+\tfrac{\bar{k}\bar{h}_w^2}{I_xI_z}\right). \end{aligned} \tag{54}$$

Note that there is no loss of generality in setting $g=\frac{\sqrt{I_x}}{\omega_o}$ and $h=\frac{\sqrt{I_xI_z}}{|\bar{h}_w|}$, since as seen in (53), g^2 and h^2 can be

absorbed by K and $\bar{k}$. We see from (54) that $k_{G\phi} \approx k_{G\psi}$, and if $I_x \approx I_z$, then additionally $k_{d\phi} \approx k_{d\psi}$. We also see that the signs of $k_{G\phi}$ and $k_{G\psi}$ depend upon $\bar{h}_w$ and $\bar{k}$. That is, both positive and negative $k_{G\phi}$ and $k_{G\psi}$ may be stabilizing.

Magnetic actuation with saturation constraints

As in the dual-spin case, we now examine the implementation of the control law (52) when using magnetic actuation under saturation constraints.

As for the dual-spin case, the control torque provided by a magnetic torquer is given by (25). Choosing the same Lyapunov-like function (17), its time-derivative along a trajectory with magnetic actuation becomes (28) with (29), where $\mathbf{T}$ in (29) is replaced by (47). As for the dual-spin case, we choose the control law to be

$$\mathbf{m} = \text{sat}\left[-\frac{K}{||\mathbf{B}||^2}\mathbf{F}(\bar{\mathbf{x}}, \tilde{h}_w, t), \mathbf{m}_{max}\right], \;\; K > 0. \tag{55}$$

Now, we keep Assumption 1, but we replace Assumption 2 with

Assumption 2'

Let $\mathbf{f}$, $\mathbf{g}$, $\mathbf{h}$, $\mathbf{i}$, $\mathbf{j} \in R^3$. Assume that at least one of $\mathbf{f}$, $\mathbf{g}$, $\mathbf{h}$, $\mathbf{i}$ or $\mathbf{j}$ is non-zero. Let $m_1 \neq 0$ and $m_2 \neq 0$ be given with $m_1 \neq m_2$. Then $\exists \epsilon > 0, \; T > 0$, such that $\forall t \geq 0$ there exists t' contained in the interval $[0, T]$ for which

$$\left|\mathbf{B}(t+t')^T \left[\mathbf{f} + \mathbf{g}\sin m_1 t' + \mathbf{h}\cos m_1 t' + \mathbf{i}\sin m_2 t' + \mathbf{j}\cos m_2 t'\right]\right| > \epsilon.$$

As an aside, note that if Assumption 2' holds, then Assumption 2 holds also.

Now, let $(\mathbf{y}(t), z(t))$ be a solution of the open-loop system

$$\begin{aligned} \dot{\mathbf{y}} &= \bar{\mathbf{A}}\mathbf{y}, \\ \dot{z} &= 0. \end{aligned} \tag{56}$$

We have seen in (50) that $\mathbf{y}(t)$ and $z(t)$ have the form

$$\begin{aligned} y_1(t) &= y_{10}\cos m_1 t + y_{20}\sin m_1 t, \\ y_2(t) &= -y_{10}\sin m_1 t + y_{20}\cos m_1 t, \\ y_3(t) &= y_{30}\cos m_2 t + y_{40}\sin m_2 t, \\ y_4(t) &= -y_{30}\sin m_2 t + y_{40}\cos m_2 t, \\ z(t) &= z_0. \end{aligned} \tag{57}$$

Substituting (57) into (29), where $\mathbf{T}$ in (29) is replaced by (47), we find that

$$\mathbf{F}\left(\mathbf{y}(t), z(t), t+t_{mj}\right) = \begin{bmatrix} F_x\left(\mathbf{y}(t), z(t), t+t_{mj}\right) \\ F_y\left(\mathbf{y}(t), z(t), t+t_{mj}\right) \\ F_z\left(\mathbf{y}(t), z(t), t+t_{mj}\right) \end{bmatrix},$$

where

$$\begin{aligned} F_x\left(\mathbf{y}(t), z(t), t+t_{mj}\right) &= W_x \mathbf{B}^T(t+t_{mj}) \left(\begin{bmatrix} 0 \\ 0 \\ -k_w z_0 \end{bmatrix} + \begin{bmatrix} 0 \\ \frac{ay_{20}}{gI_xI_z(m_2^2-m_1^2)} \\ 0 \end{bmatrix} \sin m_1 t + \begin{bmatrix} 0 \\ \frac{ay_{10}}{gI_xI_z(m_2^2-m_1^2)} \\ 0 \end{bmatrix} \cos m_1 t \right. \\ &\quad \left. + \begin{bmatrix} 0 \\ \frac{-\bar{k}ay_{40}}{hI_xI_z(m_2^2-m_1^2)} \\ 0 \end{bmatrix} \sin m_2 t + \begin{bmatrix} 0 \\ \frac{-\bar{k}ay_{30}}{hI_xI_z(m_2^2-m_1^2)} \\ 0 \end{bmatrix} \cos m_2 t \right), \end{aligned} \tag{58}$$

$$\begin{aligned} F_y\left(\mathbf{y}(t), z(t), t+t_{mj}\right) &= W_y \mathbf{B}^T(t+t_{mj}) \left(\begin{bmatrix} -\frac{ay_{20}}{gI_xI_z(m_2^2-m_1^2)} \\ 0 \\ \frac{m_1(b+I_xm_2^2)y_{10}}{gbI_x(m_2^2-m_1^2)} \end{bmatrix} \sin m_1 t + \begin{bmatrix} -\frac{ay_{10}}{gI_xI_z(m_2^2-m_1^2)} \\ 0 \\ -\frac{m_1(b+I_xm_2^2)y_{20}}{gbI_x(m_2^2-m_1^2)} \end{bmatrix} \cos m_1 t \right. \\ &\quad \left. + \begin{bmatrix} \frac{\bar{k}ay_{40}}{hI_xI_z(m_2^2-m_1^2)} \\ 0 \\ -\frac{\bar{k}m_2(b+I_xm_1^2)y_{30}}{hbI_x(m_2^2-m_1^2)} \end{bmatrix} \sin m_2 t + \begin{bmatrix} \frac{\bar{k}ay_{30}}{hI_xI_z(m_2^2-m_1^2)} \\ 0 \\ \frac{\bar{k}m_2(b+I_xm_1^2)y_{40}}{hbI_x(m_2^2-m_1^2)} \end{bmatrix} \cos m_2 t \right), \end{aligned} \tag{59}$$

$$\begin{aligned} F_z\left(\mathbf{y}(t), z(t), t+t_{mj}\right) &= W_x \mathbf{B}^T(t+t_{mj}) \left(\begin{bmatrix} k_w z_0 \\ 0 \\ 0 \end{bmatrix} + \begin{bmatrix} 0 \\ -\frac{m_1(b+I_xm_2^2)y_{10}}{gbI_x(m_2^2-m_1^2)} \\ 0 \end{bmatrix} \sin m_1 t + \begin{bmatrix} 0 \\ \frac{m_1(b+I_xm_2^2)y_{20}}{gbI_x(m_2^2-m_1^2)} \\ 0 \end{bmatrix} \cos m_1 t \right. \\ &\quad \left. + \begin{bmatrix} 0 \\ \frac{\bar{k}m_2(b+I_xm_1^2)y_{30}}{hbI_x(m_2^2-m_1^2)} \\ 0 \end{bmatrix} \sin m_2 t + \begin{bmatrix} 0 \\ -\frac{\bar{k}m_2(b+I_xm_1^2)y_{40}}{hbI_x(m_2^2-m_1^2)} \\ 0 \end{bmatrix} \cos m_2 t \right). \end{aligned} \tag{60}$$

Now, we see that $F_x\left(\mathbf{y}(t), z(t), t+t_{mj}\right)$ and $F_z\left(\mathbf{y}(t), z(t), t+t_{mj}\right)$ each contain y_{10}, y_{20}, y_{30}, y_{40}, and z_0. Therefore, assuming that Assumption 2' holds, we can make the same arguments as in the magnetically controlled dual-spin case that provided either $W_x = 1$ or $W_z = 1$, then all solutions of the closed-loop system satisfy $\left(\bar{\mathbf{x}}(t), \tilde{h}_w(t)\right) \to (\mathbf{0}, 0)$ as $t \to \infty$.

As in the dual-spin case, the control law (55) can be written as

$$\mathbf{m} = \text{sat}\left[\frac{\mathbf{W}\mathbf{B}^{\times}\boldsymbol{\tau}_{cd}}{||\mathbf{B}||^2}, \mathbf{m}_{max}\right], \tag{61}$$

where

$$\boldsymbol{\tau}_c = \begin{bmatrix} k_{G\phi}\psi - k_{d\phi}\dot{\phi} \\ -k'_w\tilde{h}_w \\ -k_{G\psi}\phi - k_{d\psi}\dot{\psi} \end{bmatrix},$$

represents the desired (ideal) control torque as in (52), and the gains are given by (53).

To summarize, we obtain the following theorem.

Theorem 5

Let Assumptions 1 and 2' hold, and let $W_x = 1$ and/or $W_z = 1$. Consider the feedback control law (61). Then, when applied to the roll/yaw and wheel error system (11), with (25) and $\mathbf{A}$ given by (42), the closed-loop system is stable and $\mathbf{x} \to \mathbf{0}$, $\tilde{h}_w \to 0$ as $t \to \infty$.

Remarks

When all three magnetic torque rods are available $\mathbf{W} = \mathbf{1}$, and when the control input is within the limits of saturation, the control laws (41) and (61) become

$$\mathbf{m} = \frac{\mathbf{B}^{\times}\boldsymbol{\tau}_{cd}}{||\mathbf{B}||^2},$$

which ensures that the actual control torque given by $\boldsymbol{\tau}_c = -\mathbf{B}^{\times}\mathbf{W}\mathbf{m}$ is the projection of the desired control torque $\boldsymbol{\tau}_{cd}$ onto the plane perpendicular to the Earth's magnetic field $\mathbf{B}$. Theorems 3 and 5 show that this implementation of the ideal control laws in (24) and (52) when using magnetic actuation yield stable and convergent closed-loop systems even when the control law saturates and/or one magnetic torque rod is disabled (two in the case of bias momentum spacecraft). Therefore, as is often done in practice [10, 11, 9], the control laws may be designed for the ideal closed-loop system with (24) or (52), and may then be implemented using (41) or (61). Closed-loop stability and convergence are then guaranteed, eliminating the need for an after the fact stability analysis (as is commonly the case [10, 11, 9]).

Note also from (28), that $\dot{V} \leq 0$ provided $\text{sign}(\{\mathbf{m}\}_i) = -\text{sign}(\{\mathbf{F}\}_i)$ for $i = x, y, z$. The control laws in (30) and (55) certainly achieve this. Therefore, the control laws remain stabilizing under the effects of control quantization.

Finally, when a full three-axis control torque is available without limitations, the closed-loop systems obtained with the control laws (24) and (52) are linear time-invariant. Now, linear time-invariant systems are convergent if and only if all closed-loop eigenvalues have negative real parts [25, p. 121]. Therefore, since the eigenvalues of a matrix are continuous functions of the matrix entries [26, p. 191], it follows that the closed-loop systems with control laws (24) and (52) are inherently robust with respect to perturbations in system parameters. We have not attempted to quantify this robustness, although techniques such as those presented in [27] could be used. Since the closed-loop systems obtained with the magnetic control laws (30) and (55) are time-varying, no such robustness claims can be

made based on the stability analyses presented in this paper. However, the Monte-Carlo type numerical simulations presented in section 5, suggest that the magnetic control laws are very robust.

5 Numerical Example

In this section, we provide a numerical example to demonstrate the theoretical results for a bias-momentum spacecraft. Fully nonlinear spacecraft attitude dynamics and kinematics are used in the simulations. The satellite parameters are

$$\begin{aligned} I_x &= 0.494034 \text{ kg}\cdot\text{m}^2, \\ I_y &= 0.56066 \text{ kg}\cdot\text{m}^2, \\ I_z &= 0.44557 \text{ kg}\cdot\text{m}^2, \\ \bar{h}_w &= -0.1 \text{ Nms}. \end{aligned}$$

The satellite is in a circular orbit of altitude 650 km, inclination 97.79^o and right ascension of ascending node 72^o. There are two active magnetic torquers, one providing a dipole moment about the spacecraft body y-axis, and the other providing a dipole moment about the body z-axis. That is, $W_x = 0$, $W_y = 1$, $W_z = 1$. The maximum capability of each magnetic torquer is 1.75 A$\cdot$m^2. A 2-1-3 Euler sequence is used to represent the spacecraft attitude relative to the local orbiting frame. Zero-mean Gaussian white noise added to each Euler angle and angular velocity measurement, with covariance 0.5 deg and 0.02 deg/s respectively. To demonstrate robustness to spacecraft inertia matrix uncertainties, the spacecraft principal axes are offset from the spacecraft body axes by a 2-1-3 Euler sequence. The spacecraft has a residual magnetic dipole given by $\mathbf{m}_{res}^T = \begin{bmatrix} 0.1 & -0.1 & 0.15 \end{bmatrix}$ A$\cdot$m^2. The Earth's magnetic field is modeled as a dipole [2, Appendix H].

The gains for the pitch control law are selected as

$$k_{pp} = 0.0019, \;\; k_{dp} = 0.0463.$$

The wheel momentum management gain is selected as $k'_w = 0.0178$. In the design of the roll/yaw gains, $K = 8.46$ and $\bar{k} = 3.82 \times 10^{-4}$ are used, resulting in gains

$$\begin{aligned} k_{G\phi} &= -1.9693 \times 10^{-4}, \\ k_{G\psi} &= -1.9778 \times 10^{-4}, \\ k_{d\phi} &= 7.4592 \times 10^{-3}, \\ k_{d\psi} &= 7.3672 \times 10^{-3}. \end{aligned}$$

As predicted by (54), we have $k_{G\phi} \approx k_{G\psi}$ and $k_{d\phi} \approx k_{d\psi}$. Therefore, in the control law implemented in this numerical example, we set $k_{G\phi} = k_{G\psi} = -2 \times 10^{-4}$ and $k_{d\phi} = k_{d\psi} = 7.5 \times 10^{-3}$.

Three separate types of simulations were performed. In the first, the gravity-gradient torque is the only external disturbance applied to the spacecraft. In the second, gravity-gradient, residual magnetic, aerodynamic and solar pressure disturbance torques are applied. The third set of simulations is a Monte-Carlo type simulation, which includes all disturbance torques.

In the first two simulations, the initial conditions are $\phi_0 = \theta_0 = \psi_0 = 10$ deg, $\dot{\phi}_0 = \dot{\theta}_0 = \dot{\psi}_0 = 0$ deg/s and $\tilde{h}_w = 0.005$ Nms. Each angle in the 2-1-3 Euler sequence representing the principal axes offset from the body axes is taken to be 10 deg.

Figures 1 to 3 show the results with only the gravity-gradient disturbance (the first simulation). Figures 1 and 2 show that as predicted by the theory, the attitude and wheel angular momentum errors converge asymptotically, even with the uncertainty in the spacecraft inertia matrix. Figure 3 shows that the magnetic torquers initially saturate when the errors are large.

Figures 4 and 5 show the results with gravity-gradient, residual magnetic, aerodynamic and solar pressure disturbance torques (the second simulation). It can be seen the attitude and wheel angular momentum errors remain bounded, showing that the control law performs well in the presence of unmodeled disturbances.

In the third set of simulations, 100 simulations were performed, with randomly generated initial attitude and wheel momentum errors, and randomly generated principal axes offset angles. The initial attitude and wheel momentum errors were taken to be normally distributed with standard deviation 3 deg (per Euler angle) and 2% respectively. The principal axes offset angles were each taken to be normally distributed with standard deviation of 3 degrees. The peak steady-state attitude and wheel momentum errors were then determined across all simulations. They were found to be 1.6113 deg (peak steady-state attitude error) and 3.8% (peak wheel momentum error).

The simulations results show that the control law is stabilizing and the closed-loop system is convergent even though the exact roll/yaw gains as derived from the stability analysis in (53) are not used, and modeling uncertainties are present, demonstrating robustness.

6 Conclusion

This paper has examined the magnetic control of dual-spin and bias momentum spacecraft, for simultaneous attitude control and momentum wheel management. The analysis in this paper has considered linearized equations of motion, such that all results obtained in this paper are local only. It is assumed in the theoretical analysis that the spacecraft principal and body axes coincide. By making suitable transformations of variables, and appropriate assumptions on the Earth's magnetic field, control laws have been derived with proven stability and asymptotic convergence in the presence of magnetic torquer saturation. Furthermore, it has been proved that in the case of a dual-spin spacecraft, only two magnetic torquers are required for the stability and convergence results to hold. In the case of a bias momentum spacecraft, stability and asymptotic convergence require only a single magnetic torquer capable of

generating a magnetic dipole moment about an axis different from the momentum wheel spin axis. Additionally, the stability analyses show that the control laws remain stabilizing under the effects of control quantization. A numerical example has been presented to demonstrate the effectiveness of the control laws and validate the theoretical results for the bias momentum spacecraft. The numerical example shows that the control laws perform well even in the presence of disturbances and spacecraft inertia matrix uncertainties.

Acknowledgements

The author gratefully acknowledges the valuable discussions and feedback from James Lee, Yuri Kim, and Alfred Ng of the Canadian Space Agency. The author also thanks the anonymous reviewers for their useful comments that helped to improve the paper.

References

[1] Sidi, M.J., *Spacecraft Dynamics and Control,* Cambridge University Press, NY, 1997.

[2] Wertz, J.R., *Spacecraft Attitude Dynamics and Control,* Dordrecht, Holland: Kluwer Academic Publishers, 1978.

[3] Stickler, A.C., Alfriend, K.T., "Elementary Magnetic Attitude Control System," *Journal of Spacecraft and Rockets*, Vol. 13, No. 5, May 1976, pp. 282–287.

[4] Hablani, H.B., "Comparative Stability Analysis and Performance of Magnetic Controllers for Bias Momentum Satellites," *Journal of Guidance, Control and Dynamics*, Vol. 18, No. 6, Nov.-Dec. 1995. pp. 1313–1320.

[5] Pittelkau, M.E., "Optimal Periodic Control for Spacecraft Pointing and Attitude Determination," *Journal of Guidance, Dynamics and Control*, Vol. 16, No. 6, Nov.-Dec. 1993, pp. 1078–1084.

[6] Lovera, M. De Marchi, E. and Bittanti, S., "Periodic attitude control techniques for small satellites with magnetic actuators," *IEEE Transactions on Control Systems Technology*, Vol. 10, 2002, pp. 90-95.

[7] Lagrasta, S., Bordin, M., "Normal Mode Magnetic Control of LEO Spacecrafts, with Integral Action," *Proc. of AIAA Guidance, Navigation and Control Conference*, San Diego, California July 29–31, 1996. Paper AIAA 96-3823.

[8] Lv, J., Ma, G., Gao, D., "Bias Momentum Satellite Magnetic Attitude Control Based on Genetic Algorithms," *Proc. of 2006 International Control Conference*, Glasgow, Scotland, United Kingdom.

[9] Silani, E. and Lovera, M., "Magnetic spacecraft attitude control: a survey and some new results," *Control Engineering Practice*, Vol. 13, 2005. pp. 357–371.

[10] Martel, F., Pal, P., Psiaki, M., "Active magnetic control system for gravity-gradient stabilized spacecraft," In *2nd annual AIAA/USU conference on small satellites*, Logan, Utah, USA, 1988.

[11] Arduini, C. Baiocco, P., "Active magnetic damping attitude control for gravity gradient stabilized spacecraft," *Journal of Guidance, Control, and Dynamics*, Vol. 20, No. 1, 1997, pp. 117-122.

[12] Wisniewski, R., "Linear Time Varying Approach to Satellite Attitude Control Using Only Electromagnetic Actuation," *Journal of Guidance, Control, and Dynamics*, Vol. 23, No. 4, 2000.

[13] Psiaki, M. L., "Magnetic Torquer Attitude Control via Asymptotic Periodic Linear Quadratic Regulation," *Journal of Guidance, Control, and Dynamics*, Vol. 24, No. 2, May 2001, pp. 386-394.

[14] Wisniewski, R. and Blanke, M., "Fully magnetic attitude control for spacecraft subject to gravity gradient," *Automatica*, Vol. 35, No. 7, 1999.

[15] Damaren, C. J., "Comments on "Fully magnetic attitude control for spacecraft subject to gravity gradient"," Automatica, Vol. 38, No. 12, 2002, pp. 2189.

[16] Lovera, M. Astolfi, A., "Global attitude regulation using magnetic control," *Proc. of 40th IEEE Conference on Decision and Control*, Orlando, Florida, December 2001.

[17] Lovera, M. Astolfi, A., "Spacecraft attitude control using magnetic actuators," *Automatica*, Vol. 40, No. 8, 2004, pp. 1405-1414.

[18] Lovera, M. Astolfi, A., "Global magnetic attitude control of spacecraft in the presence of gravity gradient," *IEEE transactions on aerospace and electronic systems*, Vol. 42, No. 3, 2006, pp. 796-805.

[19] Damaren, C. J., "Hybrid Magnetic Attitude Control Gain Selection," *Proceedings of the Institution of Mechanical Engineers, Part G: Journal of Aerospace Engineering*, Vol. 223, No. 8, 2009, pp. 1041-1047.

[20] Forbes, J.R., Damaren, C.J., "Linear Time-Varying Passivity-Based Attitude Control Employing Magnetic and Mechanical Actuation," *Journal of Guidance, Control and Dynamics*, Vol. 34, No. 5, 2011, pp. 1363–1372.

[21] de Ruiter, A.H.J., "A Fault-Tolerant Magnetic Spin Stabilizing Controller for the JC2Sat-FF Mission," *Acta Astronautica*, Vol. 68, No. 1-2, 2011, pp. 160–171.

[22] Miller, R.K., Michel, A.N., *Ordinary Differential Equations,* Dover Publications, New York, 2007.

[23] Hughes, P.C., *Spacecraft Attitude Dynamics,* Dover Publications, New York, 2004.

[24] Ogata, K., *Modern Control Engineering,* 5th Edition, Prentice-Hall, Upper Saddle River NJ, 2010.

[25] Khalil, H.K., *Nonlinear Systems,* 2nd Edition, Prentice Hall, Upper Saddle River NJ, 1996.

[26] Franklin, J.N., *Matrix Theory,* Dover Publications, New York, 1993.

[27] Wise, K.A., "Singular Value Robustness Tests for Missile Autopilot Uncertainties," *Journal of Guidance and Control*, Vol. 14, No. 3, 1991, pp. 597–606.

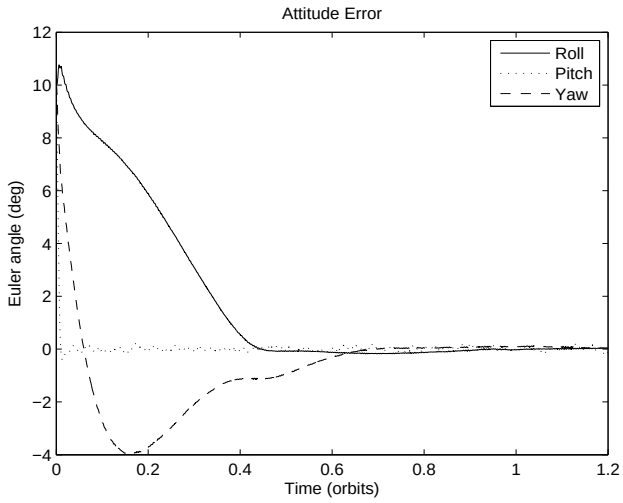

Figure 1: Spacecraft Attitude Error (Gravity-gradient disturbance only)

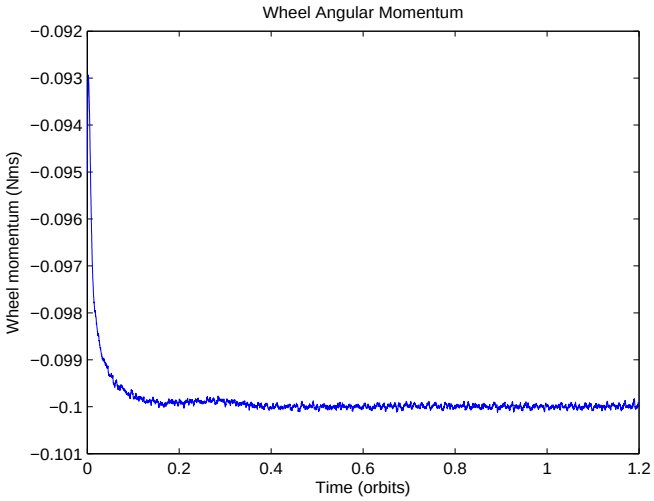

Figure 2: Wheel Angular Momentum (Gravity-gradient disturbance only)

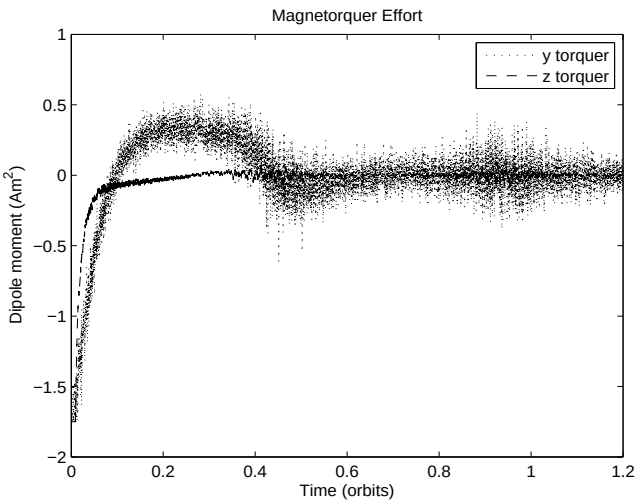

Figure 3: Magnetorquer Effort (Gravity-gradient disturbance only)

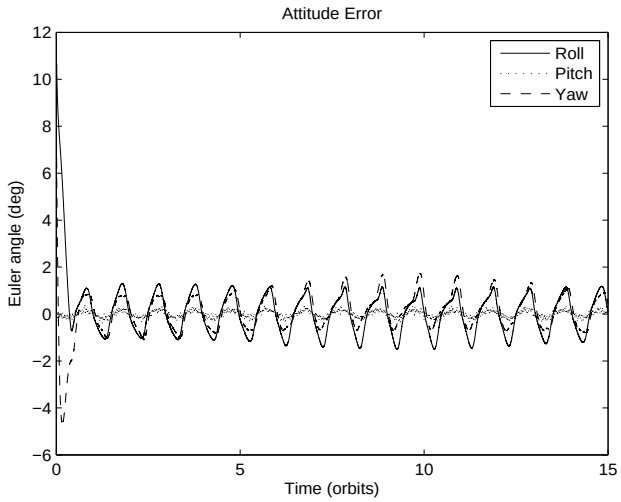

Figure 4: Spacecraft Attitude Error (All external disturbances)

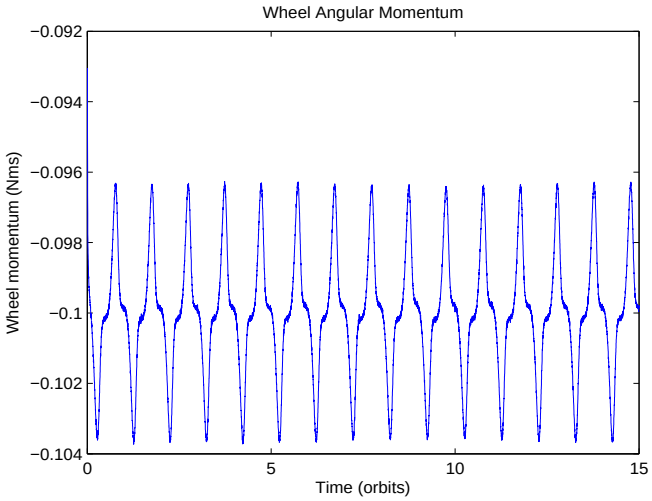

Figure 5: Wheel Angular Momentum (All external disturbances)